Carbohydrate Polymers 74 (2008) 895–900

Contents lists available at ScienceDirect

Carbohydrate Polymers

journal homepage: www.elsevier.com/locate/carbpol

Characterizations of glycerol plasticized-starch (GPS)/carbon black (CB) membranes prepared by melt extrusion and microwave radiation

Xiaofei Ma [a], Peter R. Chang [b], Jiugao Yu [a,*], Peilin Lu [a]

[a] School of Science, Tianjin University, Tianjin 300072, China
[b] Bioproducts and Bioprocesses National Science Program, Agriculture and Agri-Food Canada, 107 Science Place, Saskatoon, SK, Canada S7N 0X2

ARTICLE INFO

Article history:
Received 18 January 2008
Received in revised form 16 May 2008
Accepted 20 May 2008
Available online 28 May 2008

Keywords:
Carbon black
Electrical properties
Melt extrusion
Microwave radiation
Starch

ABSTRACT

As electrically conductive polymer composites, glycerol plasticized-starch (GPS)/carbon black (CB) membranes are respectively prepared by melt extrusion and microwave radiation. Scanning electron microscopy shows that the electrical conductance network of CB is formed in GPS/CB membranes, prepared by microwave radiation (GPS/CB-MR). However, the agglomerates of CB particles are isolated in GPS/CB membranes, prepared by melt extrusion (GPS/CB-ME). Fourier Transform Infrared (FTIR) spectroscopy reveals that CB and GPS matrix can form the interaction in GPS/CB membranes. According to Nicholais–Narkis models, the reinforcing effect of CB is more obvious in GPS/CB-MR membranes than in GPS/CB-ME membranes. GPS/CB-MR membranes exhibit a low electrical percolation threshold of 2.398 vol% CB loading and the conductivity of the membrane containing 4.236 vol% CB reaches 7.08 S/cm, while GPS/CB-ME membranes shows a very low conductivity of 10^{-8} S/cm at the high CB content. In addition, GPS/CB-MR membranes have better water vapor barrier than GPS/CB-ME membranes.

1. Introduction

Conductive polymer composites (CPC) have attracted many researches because they have potential applications such as electromagnetic shielding materials (Yang, Gupta, & Dudley, 2005) (e.g. conductive plastic films as the packaging of integrated circuit devices (Ou, Gupta, Parker, & Gerhardt, 2006)), positive temperature coefficient materials (Xu & Dang, 2007), super-capacitors for charge storage (He, Zhou, Zhou, Dong, & Li, 2004), chemical vapor detection (Chen, Hu, Hu, & Zhang, 2006), pressure sensor (Flandin, Brechet, & Cavaille, 2001) and electronic noses (Albert, Lewis, & Schauer, 2000). CPC is often composed of polymer matrix and electrically conductive fillers. Typically, the conductive fillers are metallic powders or carbonaceous fillers including carbon black, graphite, and carbon fibers (Chen, Brokken-Zijp, & Michels, 2006). Carbon black (CB) is widely used conductive filler of CPC (Yu et al., 2005). Many petroleum-based polymers (e.g. polyolefin) are applied as the matrices of CPC, because of good mechanical properties, chemical resistance and easy processing by melt extrusion. The increase in electrical conductivity is mainly ascribed to the formation of a conductive particle network in the matrix.

In recent years, natural polymers such as starch (Finkenstadt, 2005; Ma, Yu, & He, 2006, 2007), cellulose (Je & Kim, 2004), chitosan (Kim, Kim, & Kim, 2006), pectin (Sugama, 1995), hyaluronic acid (Collier, Camp, Hudson, & Schmidt, 2000), agarose and carrageenan (Ueno, Endo, Kaburagi, & Kaneko, 2004), have been used as the matrices of the solid ion-conducting composites. However, there is a few investigation about electro-conducting CPC based on natural polymer matrices. Polypyrrole is doped into poly(DL-lactide)/chitosan matrix to prepare the conductive complex membranes (Wan, Fang, & Hu, 2006). Bonnet et al. (Bonnet, Albertini, & Bizot, 2007) fabricate the films of amylose/single-walled carbon nanotubes composites, which are deposited in aqueous solutions. Glycerol plasticized-starch (GPS)/the multiwall carbon nanotube membranes are also prepared by casting method (Ma, Yu, & Wang, 2008).

Starch is an abundant, renewable, low-cost and biodegradable natural polymer. Starch-based materials can be processed easily by melt extrusion and casting. The processing methods can result in the different distribution of the filler in the matrix. The distribution of CB particles, as well as the interaction between CB and polymers has the significant effect on many properties of the CPC (Dai, Xu, & Li, 2007). In this paper, new conductive glycerol plasticized-starch (GPS)/CB membranes are prepared by an ameliorated casting method-microwave radiation (MR) and the traditional melt extrusion (ME) as the contrast. The morphology, the interaction between CB and GPS matrix, mechanical properties, electrical conductivity and water vapor permeability of GPS/CB membranes are studied.

* Corresponding author. Tel.: +86 22 27406144; fax: +86 22 27403475.
E-mail address: maxiaofei@tju.edu.cn (J. Yu).

0144-8617/$ - see front matter © 2008 Elsevier Ltd. All rights reserved.
doi:10.1016/j.carbpol.2008.05.015

2. Experimental

2.1. Materials

Cornstarch (10% moisture) is supplied by Langfang Starch Company (Langfang, Heibei, China). The sizes of the starch granules are about 20–40 μm. The plasticizer, glycerol is purchased from Tianjin Chemical Reagent Factory (Tianjin, China). Corpren® CB3000 is provided by SPC, Sweden. This grade of CB has a DBP (di-*n*-butyl phthalate) adsorption value of 380 cm^3/100 g, an iodine adsorption of 1000 mg/g and a mean particle size of 40 nm, as provided by the manufacturer.

2.2. Preparation of the membranes

2.2.1. GPS-ME and GPS/CB-ME membranes

Cornstarch, glycerol and CB particles are blended (3000 rpm, 2 min) with by use of High Speed Mixer GH-100Y, and the mixtures are stored overnight. The ratio of glycerol and cornstarch (wt./wt.) is 30:100. The mixtures are manually fed in to the single screw Plastic Extruder SJ-25(s) (Screw Ratio L/D = 25:1). The screw speed is 20 rpm. The temperature profile along the extruder barrel is 130, 140, 140 and 120 °C (from feed zone to die). The die is a 10 mm-thick metal plate with eight holes of 3 mm diameter. The extruded strips are pressed with the Flat Sulfuration Machine in to the membranes at 110 °C. GPS-ME and GPS/CB-ME membranes are obtained.

2.2.2. GPS-MR and GPS/CB-MR membranes

CB particles are dispersed into the mixture of water and glycerol (1.5 g) as a suspension using ultrasonication for 1 h. Five grams of starch is added with magnetic stirring for 1 min. The mixture is cast into a membrane on a dish. Irradiation is carried out at a 2450 MHz microwave frequency and 600 W microwave energy for 20 s in a Galanz microwave oven (Shun De, China). The formed solid-like membrane is placed in an air-circulating oven at 35 °C and 50% relative humidity (RH) until it is dry (about 4–8 h). GPS-MR and GPS/CB-MR membranes are obtained.

2.3. Scanning electron microscope (SEM)

The fracture surfaces of GPS-ME, GPS/CB-ME, GPS-MR and GPS/CB-MR membranes are performed with Scanning Electron Microscope Philips XL-3, operating at an acceleration voltage of 20 kV. These samples are frozen in liquid nitrogen, and the fracture surfaces are vacuum coated with gold for SEM.

2.4. FTIR

FTIR spectra are obtained at 2 cm^{-1} resolution with BIO-RAD FTS3000 IR Spectrum Scanner. Typically, 64 scans are signal-averaged to reduce spectral noise. The membranes are tested by attenuated total reflection measurements.

2.5. Mechanical testing

GPS/CB membranes are enveloped in a climate chamber at the conditions of 25 °C and 50% RH for one week prior to mechanical test. Testometric AX M350-10KN Materials Testing Machine is operated at a crosshead speed of 50 mm/min for tensile testing (ISO 1184–1983 standard). The data is averaged over five specimens.

2.6. Electrical conductivity

A Model ZC36 electrometer (SPSIC Huguang Instruments & Power Supply Branch, China) is used for high resistivity samples with 50 mm diameter and 0.5 mm thickness. For more conductive samples (beyond 10^{-6} S/cm) the sheets with dimensions of 30 × 5 and 0.5 mm thickness are measured using a Model ZL7 electrometer (SPSIC Huguang Instruments & Power Supply Branch, China) using a four-point test fixture.

2.7. Water vapor permeability (WVP)

Water vapor permeability (WVP) tests are carried out by ASTM method E96 (1996) with some modifications (Mali, Grossmann, Garcia, Martino, & Zaritzky, 2006). The membranes (about 0.5 mm thickness) are cut into circle shapes and sealed over with melted paraffin, stored in a desiccator at 25 °C. RH 0 is kept with anhydrous calcium chloride in the cell. And each cell is placed in a desiccator containing saturated sodium chloride to provide a constant RH 75%. Water vapor transport is determined by the weight of the permeation cell. Changes in the weight of the cell are recorded as a function of time. Slopes are calculated by linear regression (weight changes vs. time) and correlation coefficients of all reported data are >0.99. The water vapor transmission rate (*WVTR*) is defined as the slope (g/s) divided by the transfer area (m^2). *WVP* (g Pa^{-1} s^{-1} m^{-1}) is calculated as

$$\mathrm{WVP} = \frac{\mathrm{WVTR}}{P(R_1 - R_2)} \cdot D \tag{1}$$

where P is the saturation vapor pressure of water (Pa) at the test temperature (25 °C), R_1, the RH in the desiccator, R_2, the RH in the permeation cell and D is the membrane thickness (m). Under these conditions, the driving force [$P(R_1–R_2)$] is 1753.55 Pa.

3. Results and discussion

3.1. Microscopy

The morphology structure ultimately has the effect on physical properties of the polymer composites. SEM micrograph of the fractured surface of GPS-ME, GPS-MR, GPS/CB-ME and GPS/CB-MR membranes are shown in Fig. 1. Native cornstarch exists in the form of granules, while a continuous phase is formed and only a few residual small granules appear in GPS-ME and GPS-MR membranes (Fig. 1a and c). In the processing of microwave heating, due to the rapid heating rates and vibrational motion of the water molecules, the granules are subjected to a rapid increase in temperature and pressure, which results in the rapid expansion of granules. However, granular hydration fails to keep pace with granular expansion and generated resultant stress, which causes the collapse and rupture of the granules (Palav & Seetharaman, 2007). Microwave radiation produces the resultant stress in the granules, while the screw extruder provides the shear stress from the outside of granules in the processing of melt extrusion. In these two methods, because of the stress and high temperature, native cornstarch granules are molten or physically broken up, and the continuous phase (i.e. starch plasticization) is formed. As the plasticizer, glycerol plays an important role, which is known to disrupt intermolecular and intramolecular hydrogen bonds and turns granular starch into GPS (Ma, Yu, & Wan, 2006). In views of plasticization, as shown in Fig. 1a and c, microwave radiation is better than melt extrusion, because the size of residual granules is smaller in GPS-MR membranes.

In Fig. 1b and d, the distribution of CB is so different in GPS-ME and GPS-MR matrices. The connected networks of CB aggregates are basically formed in GPS/CB-MR membrane. A high-structure CB composed of many primary nanoparticles fuses together in a grape-like aggregate. And the forces from the ultrasonication can break up the agglomerates and disperse them. In the casting, the

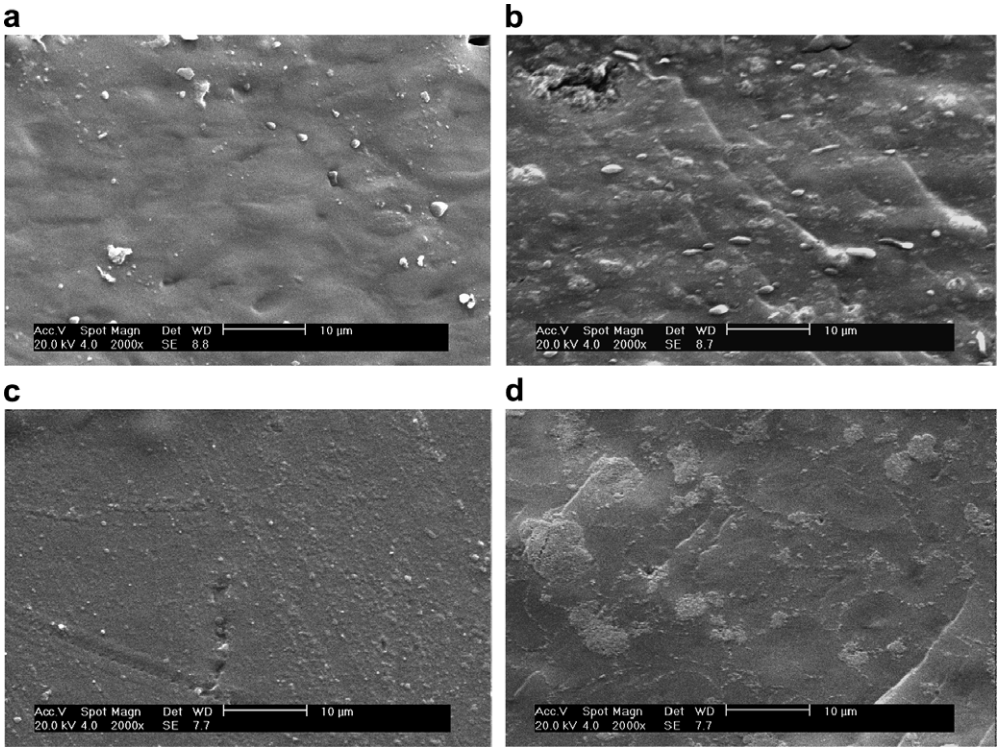

Fig. 1. SEM micrograph of GPS and GPS/CB membranes. (a) GPS-ME, (b) GPS/CB-ME membrane with 2.864 vol% CB, (c) GPS-MR, (d) GPS/CB-MR membrane with 2.864 vol% CB.

high surface tension of CB aggregates lead to flocculation in the quiescent melt (Yu et al., 2005). Flocculation makes CB particles connect with each other, and promotes the formation of a connected network, i.e. the electrical conductance network. However, melt extrusion cannot break up the agglomerates of CB particles, which are dispersed in GPS/CB-ME membrane like the islands in the sea without the connection.

3.2. FTIR

The analysis of FTIR spectra of the composites enables the interactions to be identified. If there are appreciable band shifts in the FTIR spectrum of the composites with respect to the coaddition of each component, a distinct chemical interaction (hydrogen-bonding or dipolar interaction) exists between the components (Ma, Yu, & Zhao, 2006a). On the basis of the harmonic oscillator model the reduction in force constant f can be represented by Eq. (2). (Ma, Yu, & Zhao, 2006b; Pawlak & Mucha, 2003)

$$\Delta f = f_b - f_{nb} = \frac{\mu(v_b^2 - v_{nb}^2)}{4\pi^2} \quad (2)$$

where $\mu = m_1 m_2/(m_1 + m_2)$ corresponded to the reduced mass of the oscillator, m_1 and m_2 the mass of two oscillators, υ the oscillating frequency and f the force constant. The subscripts b and nb denote bonded and non-bonded oscillators, respectively. The reduction of force constant brought about by some interaction is directly related to the frequency (or wave number) shift of stretching vibrations. For example, C and O are two oscillators in C–O group. When C–O group forms the interaction with other group (e.g. C–O···H–), the interaction between oxygen and hydrogen decreases the force constant between carbon and oxygen. As a result, the oscillating frequency of C–O group shifts to the lower wave number. According to Eq. (2), the lower the wave number corresponding to characteristic peak is, the stronger the interaction between the matrix and the filler is.

Fig. 2a and b shows the FTIR spectra of GPS/CB-ME and GPS/CB-MR membranes at room temperature in several specific stretching regions. There are two FTIR spectra regions to identify the interaction in GPS/CB membranes. The first region appears at about 3300 cm^{-1}, ascribed to the stretching peak of hydroxyl groups. The second one is composed of three characteristic peaks, ascribed to –C–O– stretching. The characteristic peak at about 1149 cm^{-1} is ascribed to C–O bond stretching of C–O–H group in GPS and two peaks at 1078 and 1016 cm^{-1} are attributed to C–O bond stretching of C–O–C group in the anhydroglucose ring of starch (Ma, Yu, & Wang, 2007).

These characteristic peaks vary with the contents of CB. As shown in Fig. 2a, when CB contents of GPS/CB-ME membranes increase from 0 to 1.928 vol%, the characteristic peaks of OH and –C–O– groups all shift towards lower wave number at two above-mentioned stretching regions. These shifts can be ascribed to the interaction between GPS matrix and CB. There are many functional polar groups like carboxylic, phenolic and lactonic on the surface of CB (Huang, 2002), which can form the interaction with OH and –C–O– groups of GPS matrix. When CB contents increase from 1.928 to 2.864 vol%, the characteristic peak of OH shift lower, but the ones of –C–O– groups shift higher wave number. It can be related to the agglomerates of CB particles, which are shown by SEM in Fig. 1b. The agglomerates actually decreases the effective contents of CB and the interaction between CB and –C–O– groups of GPS matrix. As shown in Fig. 2b, with the increasing of CB contents from 0 to 2.864 vol%, the characteristic peaks of GPS/CB-MR membranes basically shift towards lower wave number. This processing method can effectively break up the agglomerates and disperse the CB aggregates well. It is consistent with the results of SEM in Fig. 1d. Therefore, the more the CB contents are, the more the interaction of CB and GPS matrix are.

3.3. Mechanical properties

Fig. 3a and b reveal the effect of CB contents on mechanical properties of GPS/CB-ME and GPS/CB-MR membranes. As the filler of GPS matrix, CB has an obvious reinforcing effect, which increases

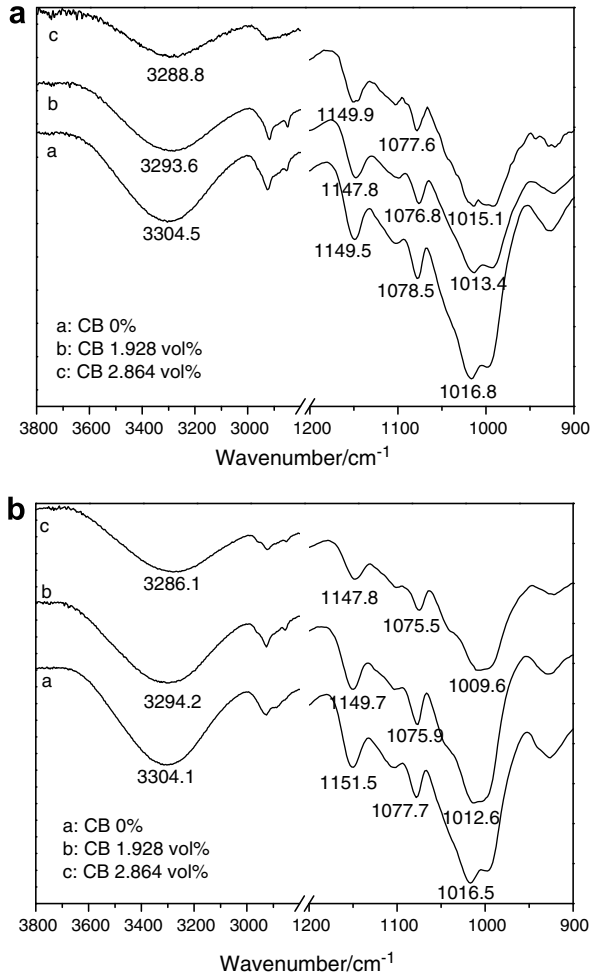

Fig. 2. FTIR spectrum of GPS/CB-ME membranes (a) and GPS/CB-MR membranes (b) with different CB contents.

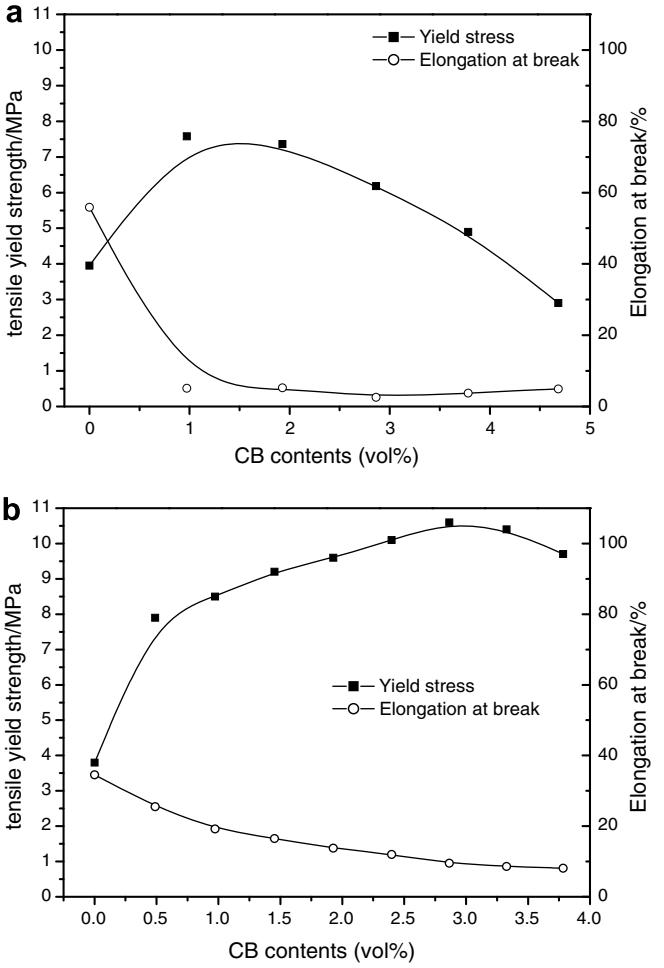

Fig. 3. The effect of CB contents on the tensile yield strength and elongation at break of GPS/CB-ME membranes (a) and GPS/CB-MR membranes (b).

the tensile yield strength in contrast with pure GPS matrix. However, with the increasing of CB contents, the elongation at break decreases. The dispersion of CB particles in GPS matrix spatially restrains the slippage movement among starch molecules, so the introduction of CB significantly decreases elongation at break of the membranes. The tensile yield strength of GPS/CB-ME membrane reaches the maximum 7.58 MPa at low filler loading of 0.973 vol%, while the tensile yield strength of GPS/CB-MR membrane reaches the maximum 10.60 MPa at higher filler loading of 2.864 vol%.

Interfacial interaction between the fillers and matrix is an important factor affecting the mechanical properties of the composites. Thus, theoretical tensile yield strength of the composites is modeled to estimate the adhesion between the filler particles and matrix. In the case of no adhesion, the interfacial layer cannot transfer stress. The tensile strengths of the composites can be predicted using Nicholais–Narkis models (Metin, Tihminlioglu, Balkose, & Ulku, 2004).

$$\sigma_c = \sigma_m(1 - a\varphi^b) \tag{3}$$

where ϕ, σ_c and σ_m are volume fraction of filler, and tensile yield strengths of the composite and matrix, respectively. In the Nicholais and Narkis model, parameters a and b are the constants related to filler-matrix interaction and geometry of the filler, respectively. The value (a) of less than 1.21 represents good adhesion for composites containing spherical fillers. In the absence of adhesion for the composites, Eq. (3) becomes

$$\sigma_c/\sigma_m = (1 - 1.21\varphi^{2/3}) \tag{4}$$

This model (Metin et al., 2004) is based on the assumption that the decrease of tensile yield strength is due to the reduction in effective cross-section area caused by the spherical filler particles. If perfect adhesion is present between the matrix and CB particles, the loading stresses will be transferred to CB, and no reduction in effective surface area will result.

The experimental and theoretical curves are plotted in Fig. 4. The experimental values of both GPS/CB-ME and GPS/CB-MR membranes are much higher than the curve calculated by Eq. (4). It indicates that there is the adhesion with some degree between the GPS matrix and CB particles. The experimental curve of GPS/CB-MR membranes is much higher than GPS/CB-ME membranes. The interaction between GPS matrix and CB particles is stronger in GPS/CB-MR membranes. CB particles act as physical cross-linking points of starch molecules, which results in the increased tensile strength. In GPS/CB-ME membranes, the agglomerates of CB particles actually decrease the effective cross-linking points and the interaction between CB and GPS matrix. It is consistent with the result of SEM and FTIR.

3.4. Electrical conductivity

Fig. 5 shows the electrical conductivity of GPS/CB membranes as a function of CB contents measured at room temperature. It is similar to the characteristic of CPC for GPS/CB-MR membranes that the

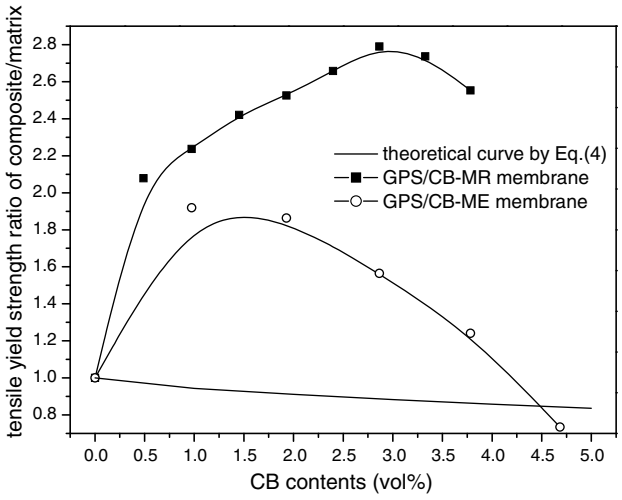

Fig. 4. The effect of CB volume fraction on yield stress ratio of the composite and matrix.

electrical conductivity increases with CB contents, raises sharply at a critical CB concentration, and tends to level off above the critical CB content. The critical concentration is usually interpreted as percolation threshold, which is required to form the interconnecting conductive networks in the polymer matrix. The percolation threshold of CB is 2.398 vol% for GPS/CB-MR membranes, at which the conductivity is increased about 7 orders of magnitude. And the conductivity of GPS/CB-MR membrane containing 4.236 vol% CB reaches 7.08 S/cm. However, the conductivity of GPS/CB-ME membranes changes a little. When CB contents increase from 0 to 4.684 vol%, the conductivity is only increased one order of magnitude. In fact, the agglomerates of CB particles are isolated, and the interconnecting conductive networks cannot form in GPS matrix. It is consistent with the morphology revealed by SEM.

According to universal percolation theory (Babinec, Mussell, Lundgard, & Cieslinski, 2000), Eq. (5) relates the conductivity (σ) of CPC to the volume fraction (ϕ) of the conductive filler in the composites above the percolation threshold (ϕ_c).

$$\sigma = \sigma_o(\varphi - \varphi_c)^t \quad (5)$$

where σ_o is a constant that is typically assigned to the plateau conductivity of the fully loaded composite, the exponent (t) fits the data and is used to interpret the mechanism of network formation. Generally, the t is about 1.1–1.3 for a two-dimensional system, while a higher value, in the range from 1.6 to 2.0 is for a three-dimensional system (Babinec et al., 2000). The t value (1.68) is obtained from the slope of the line in a $\log(\varphi - \varphi_c)$ vs. $\log\sigma$ plot in Fig. 6. The $\log(\varphi - \varphi_c)$ vs. $\log\sigma$ plot of GPS/CB-MR membranes exhibits a good linearity (R = 0.989). The t value of GPS/CB-MR membranes is in the range from 1.6 to 2.0, indicating that the three-dimensional conductive networks are formed.

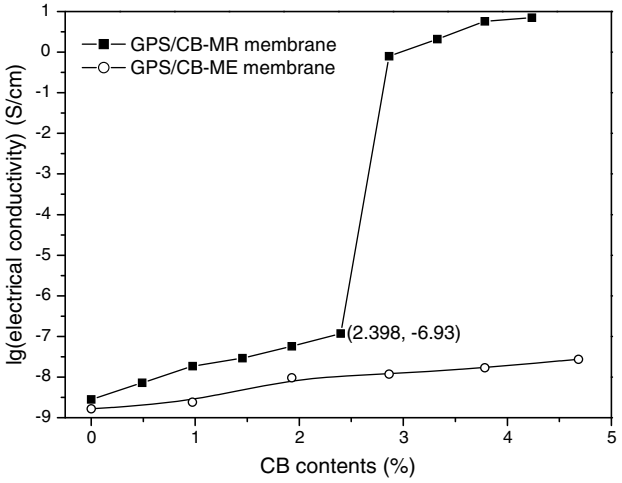

Fig. 5. The electrical conductivity of GPS/CB membranes with different CB contents.

3.5. Water vapor permeability (WVP)

Hydrophilic starch-based materials are sensitive to water vapor. Water vapor permeability (WVP) is often used to study the moisture transport through the membrane. As shown in Fig. 7, with the increasing of CB contents, WVP values of GPS/CB-MR membranes obviously decrease, then change gradually. When CB contents are more than the percolation thresholds, WVP values changed less at about 2.84×10^{-1} g m^{-1} s^{-1} Pa^{-1}. With the increasing of CB contents, WVP values of GPS/CB-ME membranes decrease gradually from 5.83×10^{-1} to 3.31×10^{-10} g m^{-1} s^{-1} Pa^{-1}. The addition of CB introduces a tortuous path for diffusing water vapor (Kristo & Biliaderis, 2007). The reduction of WVP values arises from the longer diffusive path, through which water vapor must travel in the presence of CB (Ray & Okamoto, 2003). When the CB connected networks are formed in GPS/CB-MR membranes, superfluous agglomerates of CB actually decrease the effective contents of CB and make WVP of GPS/CB-MR membranes decrease less. GPS/CB-MR membranes have better water vapor barrier than GPS/CB-ME membranes because the good dispersion of CB in GPS/CB-MR membranes lead to the reduction of permeability.

4. Conclusion

In this paper, GPS/CB membranes are fabricated by microwave radiation and melt extrusion. Microwave radiation is a more effective method to prepare GPS/CB membranes than melt extrusion. Microwave radiation makes CB particles connect with each other, and forms the electrical conductance network. However, melt extrusion cannot break up the agglomerates of CB particles, which are isolated in GPS matrix. The hydroxyl and –C–O– groups of GPS matrix can form the interaction with CB. The interaction between GPS matrix and CB particles is stronger for GPS/CB-MR membranes than GPS/CB-ME membranes. The maximal tensile yield strength of GPS/CB-MR membranes reaches 10.60 MPa, while the one of GPS/CB-MR membranes is only 7.58 MPa. As predicated by universal

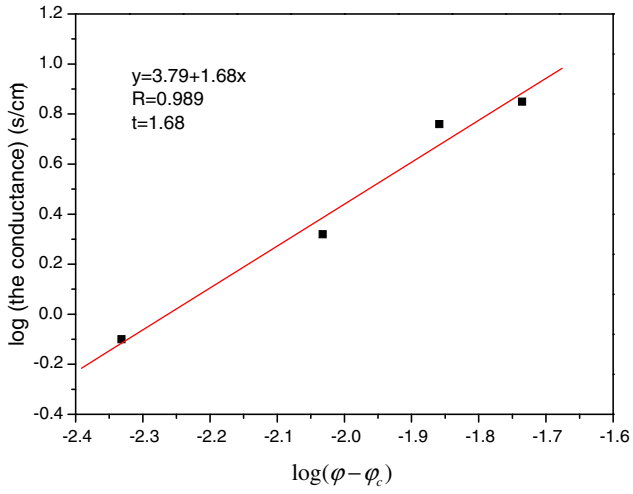

Fig. 6. Electrical conductivity as a function of excess concentration ($\varphi - \varphi_c$) for GPS/CB-MR membranes.

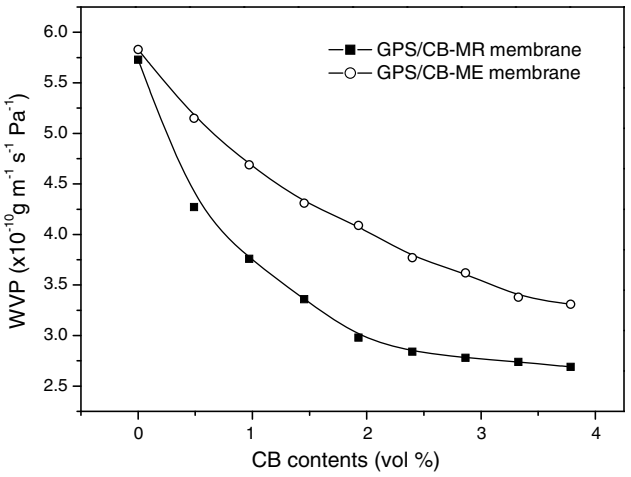

Fig. 7. The effect of CB on water vapor permeability of GPS/CB membranes.

percolation theory, GPS/CB-MR membranes forms the three-dimensional conductive networks at a low electrical percolation threshold of 2.398 vol% CB loading and the conductivity of the membrane containing 4.236 vol% CB is 7.08 S/cm. In contrast, GPS/CB-ME membranes have a very low electrical conductivity (10^{-8} S/cm). And GPS/CB-MR membranes exhibit better water vapor barrier than GPS/CB-ME membranes.

References

Albert, K. J., Lewis, N. S., & Schauer, C. L. (2000). Cross-reactive chemical sensor arrays. *Chemical Reviews, 100*, 2595–2626.

Babinec, S. J., Mussell, R. D., Lundgard, R. L., & Cieslinski, R. (2000). Electroactive thermoplastics. *Advanced Materials, 12*, 1823–1834.

Bonnet, P., Albertini, D., & Bizot, H. (2007). Amylose/SWNT composites: From solution to film-synthesis, characterization and properties. *Composites Science and Technology, 67*, 817–821.

Chen, S. G. Z., Brokken-Zijp, X. L. J. C. M., & Michels, J. M. A. J. (2006) Novel phthalocyanine crystals as a conductive filler in crosslinked epoxy materials: Fractal particle networks and low percolation thresholds. *Journal of Polymer Science Part B – Polymer Physics, 44*, 33–47.

Chen, Z. S. G., Hu, J. C. M. X. L., Hu, J. , & Zhang, M. A. J. M. Q. (2006). Relationships between organic vapor adsorption behaviors and gas sensitivity of carbon black filled waterborne polyurethane composites. *Sensors and Actuators B – Chemical, 119*, 110–117.

Collier, J. H., Camp, J. P., Hudson, T. W., & Schmidt, C. E. (2000). Synthesis and characterization of polypyrrole-hyaluronic acid composite biomaterials for tissue engineering applications. *Journal of Biomedical Materials Research, 50*, 574–584.

Dai, K., Xu, X. B., & Li, Z. M. (2007). Electrically conductive carbon black (CB) filled in situ microfibrillar poly(ethylene terephthalate) (PET)/polyethylene (PE) composite with a selective CB distribution. *Polymer, 48*, 849–859.

Finkenstadt, J. Y. (2005). Natural polysaccharides as electroactive polymers. *Applied Microbiology and Biotechnology, 67*, 735–745.

Flandin, V. L. L., Brechet, Y., & Cavaille, J. Y. (2001). Electrically conductive polymer nanocomposites as deformation sensors. *Composites Science and Technology, 61*, 895–901.

He, B. L., Zhou, Y. K., Zhou, W. J., Dong, B., & Li, H. L. (2004). Preparation and characterization of ruthenium-doped polypyrrole composites for supercapacitor. *Materials Science and Engineering A, 374*, 322–326.

Huang, J. C. (2002). Carbon black filled conducting polymers and polymer blends. *Advanced Polymer Technology, 21*, 299–313.

Je, C. H., & Kim, K. J. (2004). Cellophane as a biodegradable electroactive polymer actuator. *Sensors and Actuators A – Physical, 112*, 107–115.

Kim, S. J., Kim, M. S., & Kim, S. I. (2006). Self-oscillatory actuation at constant DC voltage with pH-sensitive chitosan/polyaniline hydrogel blend. *Chemistry of Materials, 18*, 5805–5809.

Kristo, E., & Biliaderis, C. G. (2007). Physical properties of starch nanocrystal-reinforced pullulan films. *Carbohydrate Polymers, 68*, 146–158.

Ma, X. F., Yu, J. G., & He, K. (2006). Thermoplastic starch plasticized by glycerol as solid polymer electrolytes. *Macromolecular Materials and Engineering, 291*, 1407–1413.

Ma, X. F., Yu, J. G., & He, K. (2007). The effects of different plasticizers on the properties of thermoplastic starch as solid polymer electrolytes. *Macromolecular Materials and Engineering, 292*, 503–510.

Ma, X. F., Yu, J. G., & Wan, J. J. (2006). Urea and ethanolamine as a mixed plasticizer for thermoplastic starch. *Carbohydrate Polymers, 64*, 267–273.

Ma, X. F., Yu, J. G., & Wang, N. (2007). Production of thermoplastic starch/mmt-sorbitol nanocomposites by dual-melt extrusion processing. *Macromolecular Materials and Engineering, 292*, 723–728.

Ma, X. F., Yu, J. G., & Wang, N. (2008). Glycerol plasticized-starch/multiwall carbon nanotube composites for electroactive polymers. *Composites Science and Technology, 68*, 268–273.

Ma, X. F., Yu, J. G., & Zhao, A. (2006a). Compatibility characterization of poly(lactic acid)/poly(propylene carbonate) blends. *Journal of Polymer Science Part B – Polymer Physics, 44*, 94–101.

Ma, X. F., Yu, J. G., & Zhao, A. (2006b). Properties of biodegradable poly(propylene carbonate)/starch composites with succinic anhydride. *Composites Science and Technology, 66*, 2360–2366.

Mali, S., Grossmann, M. V. E., Garcia, M. A., Martino, M. N., & Zaritzky, N. E. (2006). Effects of controlled storage on thermal, mechanical and barrier properties of plasticized films from different starch sources. *Journal of Food Engineering, 75*, 453–460.

Metin, D., Tihminlioglu, F., Balkose, D., & Ulku, S. (2004). The effect of interfacial interactions on the mechanical properties of polypropylene/natural zeolite composites. *Composites Part A, 35*, 23–32.

Ou, R. Q., Gupta, S., Parker, C. A., & Gerhardt, R. A. (2006). Fabrication and electrical conductivity of poly(methyl methacrylate) (PMMA)/carbon black (CB) composites: Comparison between an ordered carbon black nanowire-like segregated structure and a randomly dispersed carbon black nanostructure. *Journal of Physical Chemistry B, 110*, 22365–22373.

Palav, T., & Seetharaman, K. (2007). Impact of microwave heating on the physico-chemical properties of a starch–water model system. *Carbohydrate Polymers, 67*, 596–604.

Pawlak, A., & Mucha, M. (2003). Thermogravimetric and FTIR studies of chitosan blends. *Thermochimica Acta, 396*, 153–166.

Ray, S., & Okamoto, M. (2003). Polymer/layered silicate nanocomposites: A review from preparation to processing. *Progress in Polymer Science, 28*, 1539–1641.

Sugama, T. (1995). Pectin copolymers with organosiloxane grafts as corrosion-protective coatings for aluminum. *Materials Letters, 25*, 291–299.

Ueno, H., Endo, Y., Kaburagi, Y., & Kaneko, M. (2004). New ionically conductive solids of polysaccharides containing excess water. *Journal of Electroanalytical Chemistry, 570*, 95–100.

Wan, Y., Fang, Y., & Hu, Z. L. (2006). Electrically conductive poly(DL-lactide)/chitosan/polypyrrole complexes. *Macromolecular Rapid Communications, 27*, 948–954.

Xu, H. P., & Dang, Z. M. (2007). Electrical property and microstructure analysis of poly(vinylidene fluoride)-based composites with different conducting fillers. *Chemical Physics Letters, 438*, 196–202.

Yang, Y. L., Gupta, M. C., & Dudley, K. L. (2005). Conductive carbon nanoriber-polymer foam structures. *Advanced Materials, 17*, 1999–2003.

Yu, J., Zhang, L. Q., Rogunova, M., Summers, J., Hiltner, A., & Baer, E. (2005). Conductivity of polyolefins filled with high-structure carbon black. *Journal of Applied Polymer Science, 98*, 1799–1805.